Scattering of 22-MeV Alpha Particles by Fe^{56}, Zn^{64}, Zn^{66}, and Zn^{68}†

H. L. WILSON AND M. B. SAMPSON
Indiana University, Bloomington, Indiana
(Received 22 June 1964)

Angular distributions for elastic scattering and for inelastic scattering to the lowest 2^+ and 3^- states in Fe^{56}, Zn^{64}, Zn^{66}, and Zn^{68} have been measured using 22.2-MeV alpha particles. The elastic distributions extend from 20 to 167° and the 2^+ distributions from 30 to 167°. The 3^- distribution extends from 30 to 107° for Fe^{56}, whereas for the Zn isotopes the range is from 60 to 167°. The optical model has been used to fit the elastic-scattering distributions, and the parameters thus found have been used in fitting the 2^+ distributions using a distorted wave Born approximation calculation. Three sets of optical-model parameters were found that would fit the elastic scattering distributions (for $\Theta \leq 125°$). The real parts of the optical-model potential for these three sets are $V_0 = -20$, -40, and -70 MeV. It was found that only the set with $V_0 = -20$ MeV also gave good fits to the 2^+ distributions. For $\Theta > 125°$, the fits were found to be quite poor. Two suggestions have been made to explain the failure of the theory at such large scattering angles. Nuclear deformabilities obtained by fitting the inelastic 2^+ data are in good agreement with those obtained by inelastic proton scattering and electromagnetic methods. Approximations and limitations associated with the theoretical interpretation are discussed.

I. INTRODUCTION

CONSIDERABLE success has been obtained within the framework of the optical model in analyzing the elastic scattering of medium- and high-energy (10–50 MeV) alpha particles, deuterons, and nucleons.[1–8] It is found, however, that the parameters required to fit the data for strongly absorbed particles are not unique. In particular, as a result of an optical-model analysis of elastic alpha-particle scattering,[1] Igo[9] has proposed that the scattering is dependent only on the surface of the nucleus. This can be expressed by the invariance conditions

$$V_0 \exp(R_0/d) = C_1, \quad (1)$$

$$W_0 \exp(R_0'/d') = C_2, \quad (2)$$

where V_0 is the depth of the real part and W_0 the depth of the imaginary part of the optical potential and R_0, R_0', and d,d' are the radii and diffuseness parameters of the real and imaginary wells, respectively, while C_1 and C_2 are constants. This implies that once C_1 and C_2 are known an infinite set of parameters can be generated which will fit the elastic data equally well.

Austern[10] has shown, on the basis of a WKB calculation, that Igo's suggestion is an oversimplification and that it is indeed possible for the nuclear interior to influence the scattering. This conclusion is confirmed by Drisko *et al.*[11] who fit the experimental elastic-scattering data for 43-MeV alpha particles on Ni^{58}. They show that the conditions expressed by Eqs. (1) and (2) must be modified to allow only discrete values of V_0 and W_0. Evidence is also obtained from the elastic scattering of 11.8-MeV deuterons by Zr, which further confirms Austern's results. In fact, these authors conclude that the influence of the nuclear interior depends on the wavelength λ, of the incident particle, becoming more important as λ increases. For 22.2-MeV alpha particles incident on nuclei in the Fe, Zn region $\lambda \approx 0.5$ F, whereas for 43-MeV alpha particles on Ni, $\lambda \approx 0.37$ F. One would therefore expect the interior of the nucleus to have a greater effect at 22.2 MeV than at 43 MeV.

One value of this experimental data is to show, first, that an ambiguity in the optical-model potential arises when the elastic scattering of 22.2-MeV alpha particles is analyzed and, second, that this ambiguity can be reduced by analysis of the inelastic 2^+ data.

II. EXPERIMENTAL

A. General

The experimental arrangement for measuring the angular distributions was similar to that previously used[12] in the study of C^{12}. The external beam of 22.2-MeV alpha particles from the Indiana University cyclotron, focused and defined in energy by a system of quadrupole and bending magnets, was used in conjunction with the 16-in. scattering chamber. The scattered particles were detected with an Ortec surface-barrier solid-state counter and the pulses analyzed with a Nuclear Data 1024 channel analyzer. The charge passing through the target was measured with a calibrated Faraday-cup system.

* Work supported by the National Science Foundation.
[1] G. Igo and R. M. Thaler, Phys. Rev. **106**, 126 (1957).
[2] M. A. Melkanoff, J. C. Nodvik, D. S. Saxon, and R. D. Woods, Phys. Rev. **106**, 793 (1957).
[3] W. B. Cheston and A. E. Glasgold, Phys. Rev. **106**, 1215 (1957).
[4] E. C. Holbert, R. H. Bassel, and G. R. Satchlen, Bull. Am. Phys. Soc. **1**, 357 (1962).
[5] C. M. Perey and F. G. Perey, Phys. Rev. **132**, 755 (1963).
[6] F. Perey, Phys. Rev. **131**, 745 (1963).
[7] E. C. Halbert, Nucl. Phys. **50**, 353 (1964).
[8] M. A. Melkanoff, T. Sawada, and N. Cindro, Phys. Letters **2**, 98 (1962).
[9] G. Igo, Phys. Rev. Letters **1**, 72 (1958).
[10] N. Austern, Ann. Phys. **15**, 299 (1961).
[11] R. M. Drisko, G. R. Satchler, and R. H. Bassel, Phys. Letters **5**, 347 (1963).
[12] R. A. Atneosen, H. L. Wilson, M. B. Sampson, and D. W. Miller (to be published).

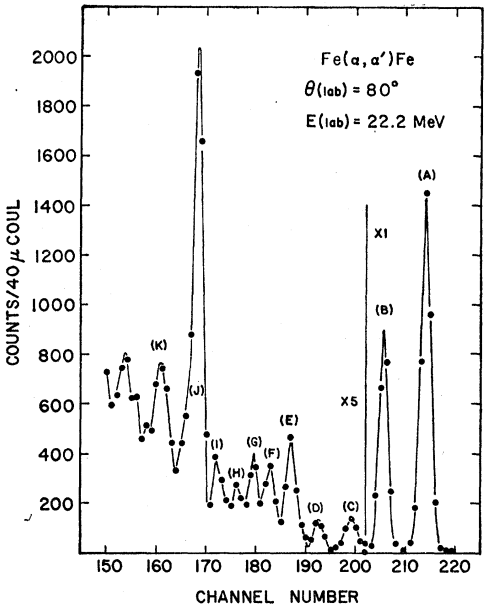

FIG. 1. Pulse-height spectrum of alpha particles scattered at 80° (lab) by a natural Fe target (92% Fe^{56}). The Q values of the lettered groups are given in Table II.

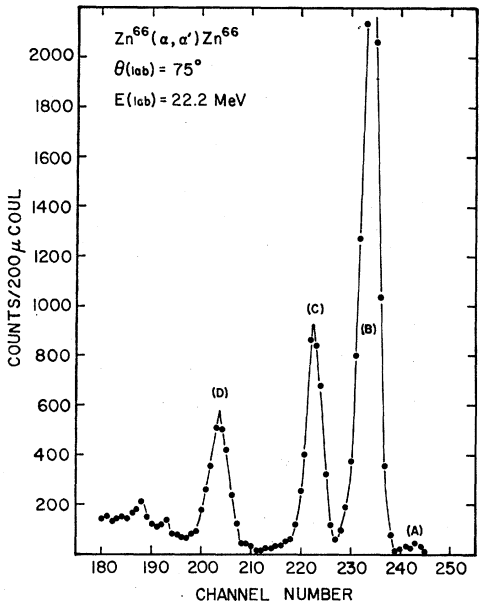

FIG. 3. Pulse-height spectrum of alpha particles scattered at 75° (lab) by Zn^{66}. The Q values of the lettered groups are given in Table II.

B. Targets

The particular target nuclei used in this experiment were selected because the optical model has been quite successful in the Fe-Zn region and also because Fe^{56} and the three zinc isotopes studied are good collective model nuclei.

The zinc targets used in this experiment were prepared by vacuum evaporation of separated isotopes. Considerable difficulty was encountered in getting the zinc to condense on the Formvar backing. This trouble was overcome by first evaporating a very thin (monatomic or less) layer of silver onto the backing. The zinc was then evaporated onto the backing with the silver atoms apparently serving as condensation centers.

The results of the target thickness measurements are presented in Table I. These values (except for Fe) were

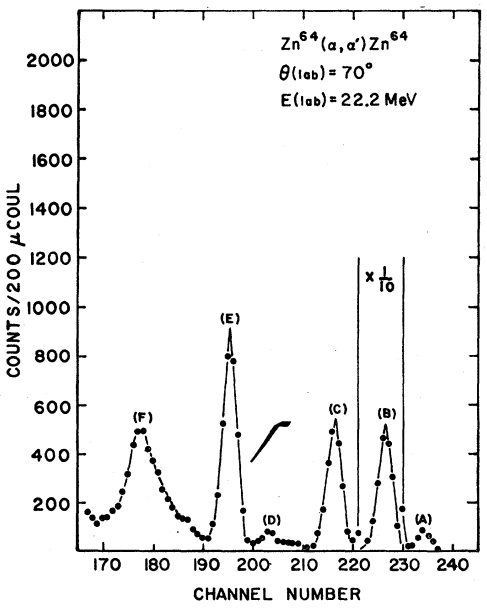

FIG. 2. Pulse-height spectrum of alpha particles scattered at 70° (lab) by Zn^{64}. The Q values of the lettered groups are given in Table II.

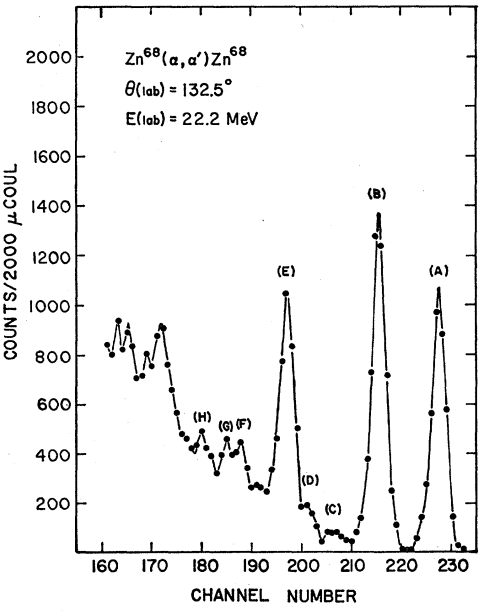

FIG. 4. Pulse-height spectrum of alpha particles scattered at 132.5° (lab) by Zn^{68}. The Q values of the lettered groups are given in Table II.

obtained by measuring the energy loss of 8.78 MeV Th C' alpha particles in the target. This energy loss was then converted to thickness by use of the atomic stopping cross sections.[13] The thickness of the iron target (92% Fe^{56}) was obtained by weighing. In all cases the contaminants were determined at an angle (about 85°) where their elastic-scattering peaks were well separated from each other and from the zinc or iron peaks of interest. The number of counts under each contaminant elastic peak was then determined and, since the relevant differential cross sections were available,[12,14] the contaminant abundances could readily be calculated. Oxygen and carbon were present in the zinc targets because of the Formvar backing while only oxygen was present in the iron target.

III. DATA ANALYSIS AND EXPERIMENTAL RESULTS

A. Group Identification

With the exception of the ground state and first two excited states, the levels in all isotopes studied in this experiment lie quite close together. This is especially true for Fe^{56}. Also, the iron target was of such a thickness that the energy lost in the target by the scattered particles made the identification of groups corresponding to highly excited states impossible. To facilitate the identification of these lower energy groups, a computer program was written which took into account the following effects:

(1) The energy dependence of the stopping cross section per atom.

(2) The effective target thickness as a function of scattering angle.

For a given scattering angle, the object of the program was to compute the energies of the scattered particles, as seen by the counter, for each Q value. The Q values for the zinc isotopes were taken from the Nuclear Data Sheets; those for Fe^{56} were taken from Aspinall *et al.*[15] A knowledge of the number of channels between the ground-state group and the group from the first excited state, made it possible to obtain a calibration. The calibration then allowed the identification of each group with the proper Q value. This procedure was carried out at five angles spaced about 20°. Typical spectra are illustrated in Figs. 1 through 4. The spectra for Fe, Zn^{64}, and Zn^{66} were selected so that the peaks of interest would not be obscured by the elastic scattering of the contaminants. The Zn^{68} spectrum was chosen as representative of the back-angle spectra. The Q values corresponding to the lettered peaks are given in Table II.

TABLE I. Target thicknesses.

Target	Primary constituent	Thickness (μg/cm^2) Contaminants
Zn^{64}	Zn^{64}(251)	O^{16}(7.4), C^{12}(14.6)
Zn^{66}	Zn^{66}(334)	O^{16}(11.1), C^{12}(20.7)
Zn^{68}	Zn^{68}(396)	O^{16}(5.5), C^{12}(14.2)
Fe	Fe^{56}(1340)	O^{16}(10.4)

TABLE II. The nuclear states.

Target	Letter	Spin and parity[a]	$-Q$(MeV)	
Fe	A	0^+	0.0	Fe
	B	2^+	0.842	Fe^{56}
	C	2^+	1.41	Fe^{54}
	D	4^+	2.079	Fe^{56}
	E	2^+	2.652	
	F	2^+	2.955	
	G		3.365	
	H		3.819	
	I		4.108	
	J	3^-	4.387	
	K		5.13	
Zn^{64}	A		0.0	Ag
	B	0^+	0.0	Zn^{64}
	C	2^+	0.99	
	D	(4^+)	2.27	
	E	3^-	3.04	
	F	0^+	0.0	O^{16}
Zn^{66}	A		0.0	Ag
	B	0^+	0.0	Zn^{66}
	C	2^+	1.04	
	D	3^-	2.76	
Zn^{68}	A	0^+	0.0	Zn^{68}
	B	2^+	1.08	
	C	(2^+)	1.89	
	D	2^+	2.32	
	E	3^-	2.68	
	F		3.47	
	G		3.80	
	H		4.10	

[a] A parenthesis around a spin assignment means that the assignment is uncertain.

B. Cross-Section Determination

The conversion from the multichannel analyzer output to a differential cross section is a straightforward but laborious task. This was particularly true in this experiment, where background subtractions were made over large angular ranges. In an effort to be as consistent as possible, all the data were plotted and the background subtracted.

Before the final numbers were obtained it was necessary to normalize all the data to one counter collimator. Three different collimators were used for the zinc distributions. The smallest, a $\frac{1}{16}$ in. hole with solid angle $(0.32\pm0.01)\times10^{-3}$ sr, was used at angles less than 50°, to keep the analyzer dead time at a reasonable value. A $\frac{1}{16}$ in. slit with solid angle $(1.99\pm0.04)\times10^{-3}$ sr was used from 50° to 100°. At approximately 100°, the target was rotated from transmission to reflection

[13] W. Whaling, *Handbuch der Physik*, edited by S. Flügge (Springer-Verlag, Berlin, 1958), Vol. 34, pp. 193–217.

[14] J. G. Cramer, Jr. and W. W. Eidson, Bull. Am. Phys. Soc. 8, 317 (1963).

[15] A. Aspinall, G. Brown, and S. E. Warren, Nucl. Phys. 46, 33 (1963).

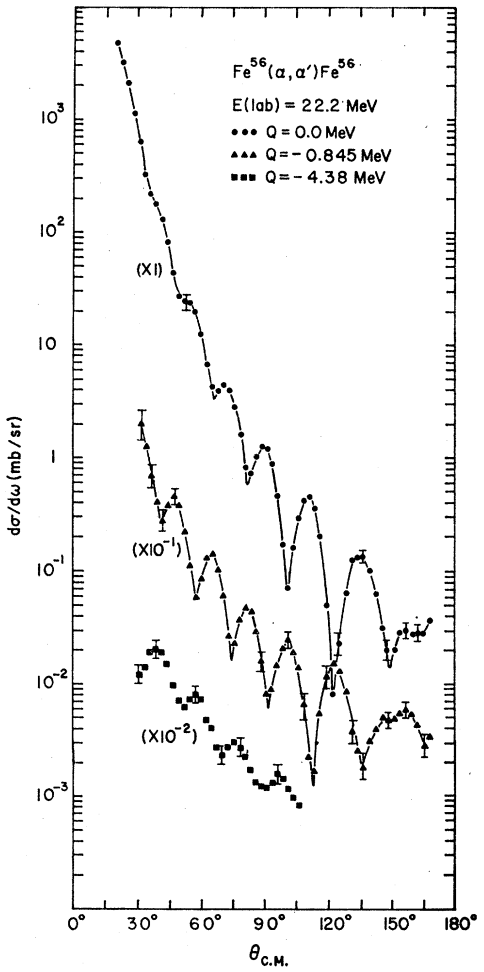

FIG. 5. Differential cross sections for elastic scattering and for excitation of the levels at 0.845 and 4.38 MeV in Fe^{56} by 2.2-MeV alpha particles.

and the $\frac{1}{16}$ in. slit replaced with a $\frac{1}{8}$ in. slit for the remaining angles. The normalizations at 50 and 100° were made by measuring four angles with both slits. This made it possible to find the solid-angle ratios under actual experimental conditions. The absolute values of the solid angles were then determined by a careful geometric measurement. Two collimators were used in obtaining the Fe^{56} distributions. The $\frac{1}{8}$ in. slit was not needed with the thicker target.

The numbers resulting from the data reduction, i.e., with all normalizations and corrections made, were then converted to differential cross sections using the Indiana University IBM 709 computer. The ratio of the elastic differential cross section to the Rutherford cross section was also computed for each elastic distribution. Representative experimental angular distributions for Fe^{56}, Zn^{64}, Zn^{66}, and Zn^{68} are illustrated in Figs. 5 through 8, respectively. In these figures, all error bars represent relative errors except the one at about 50° on the elastic distributions which represents the uncertainty in the over-all normalization.

IV. THEORETICAL ANALYSIS OF THE DATA

A. Fitting Procedure

In the introduction it was mentioned that Igo, as a result of optical-model analyses of elastic alpha-particle scattering data, has attributed the scattering strictly to the nuclear surface. This is expressed by the invariance conditions given in Eqs. (1) and (2). If one set of parameters can be found to fit the elastic data, these parameters can then be used to determine the constants C_1 and C_2. Equations (1) and (2) can then be used to generate a family of sets of parameters that should fit the elastic data equally well. However, Eq. (2) is not well established[11] so that in the calculations reported here, R_0' and d' were set equal to R_0 and d, respectively. Instead of using Eq. (2) to determine W_0, a scan was

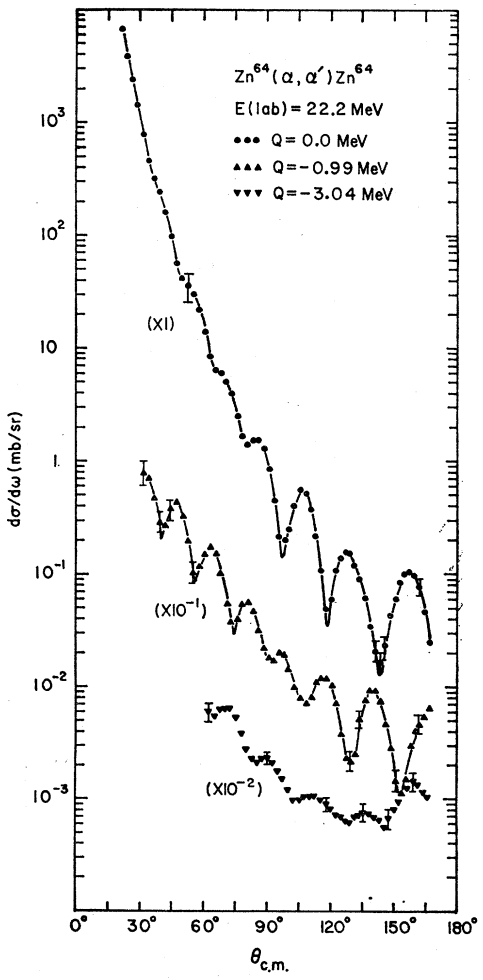

FIG. 6. Differential cross sections for elastic scattering and for excitation of the levels at 0.99 and 3.04 MeV in Zn^{64} by 22.2-MeV alpha particles.

therefore done over W_0 until a minimum in the quantity χ^2 was found, where

$$\chi^2=\sum_{i=1}^{N}\left[\frac{\sigma_T(\Theta_i)-\sigma_E(\Theta_i)}{\sigma_E(\Theta_i)}\right]^2. \quad (3)$$

In this equation $\sigma_T(\Theta_i)$ is the theoretically predicted elastic scattering cross section at angle Θ_i and $\sigma_E(\Theta_i)$ is the corresponding experimental result. Θ_N in all cases is about 120°. Thus χ^2 (together with a visual examination) is a measure of the "goodness of fit" in the range from 20 to 120°. Setting R_0' and d' equal to R_0 and d, respectively, simplifies the computations since only one form factor need be calculated. The optical potential used in the calculations is of the Woods-Saxon type, namely,

$$V=(V_0+iW_0)\{1+\exp[(r-R)/d]\}^{-1}, \quad (4)$$

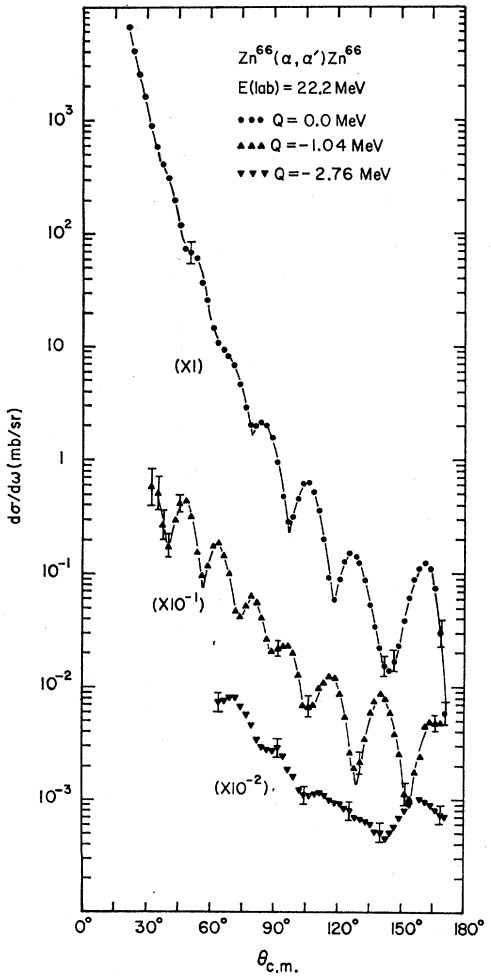

FIG. 7. Differential cross sections for elastic scattering and for excitation of the levels at 1.04 and 2.76 MeV in Zn^{66} by 22.2-MeV alpha particles.

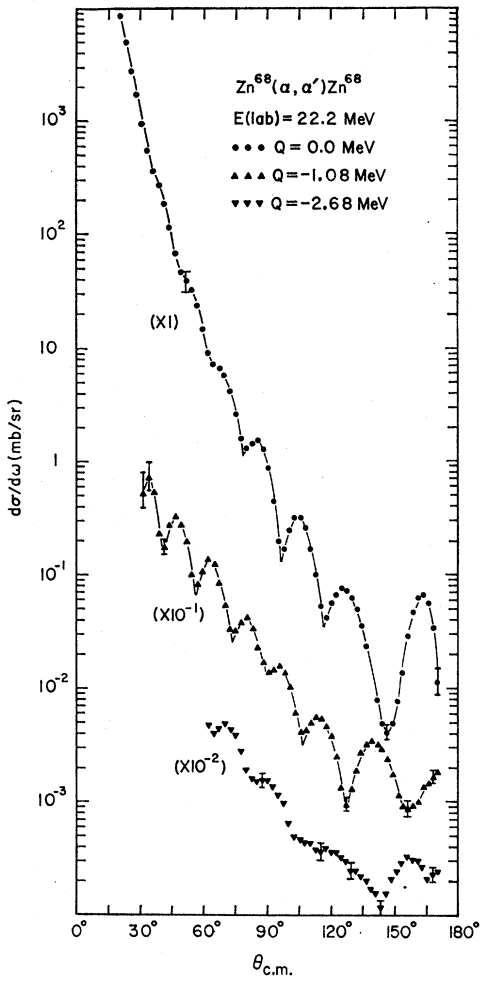

FIG. 8. Differential cross sections for elastic scattering and for excitation of the levels at 1.08 and 2.68 MeV in Zn^{68} by 22.2-MeV alpha particles.

where

$$R=R_0\left(1+\sum_{\mu=-2}^{2}\alpha_{2\mu}{}^*Y_{2\mu}(\Theta,\Phi)\right). \quad (5)$$

The $\alpha_{2\mu}{}^*$ are the dynamical variables which describe the nuclear surface and in terms of which the nuclear Hamiltonian H_N for the quadrupole, harmonic, vibrational model can be written[16] as

$$H_N(\alpha)=\sum_{\mu=-2}^{2}\tfrac{1}{2}B_2|\pi_{2\mu}|^2+\tfrac{1}{2}C_2|\alpha_{2\mu}|^2, \quad (6)$$

where the $\pi_{2\mu}$ are the momenta conjugate to the $\alpha_{2\mu}$. In the calculations reported in this paper, V was expanded in a Taylor series about the point $R=R_0$. Thus

$$V=V(r-R_0)-\left.\frac{\partial V}{\partial r}\right|_{R=R_0}\sum_{\mu=-2}^{2}\alpha_{2\mu}{}^*Y_{2\mu}(\Theta,\Phi)+\cdots. \quad (7)$$

[16] K. Alder, A. Bohr, T. Haas, B. Mottelson, and A. Winther, Rev. Mod. Phys. **28**, 432 (1956).

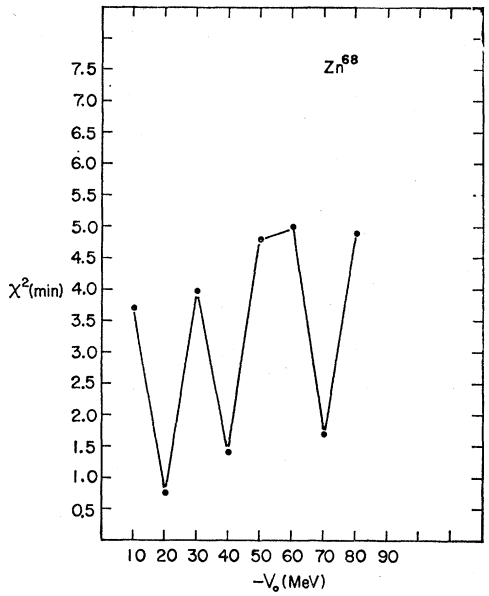

FIG. 9. Plot of χ^2 (min) versus $-V_0$, the real part of the optical potential, for Zn^{68}.

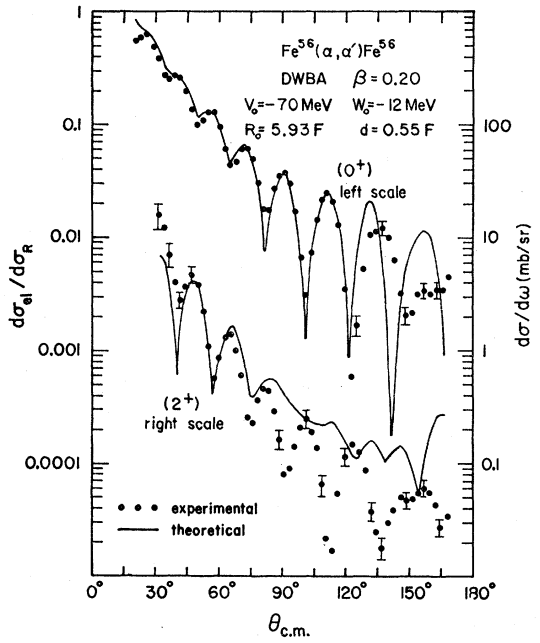

FIG. 11. Experimental and theoretical ($V_0=-40$ MeV) angular distributions for the reaction $Fe^{56}+\alpha$(22.2 MeV).

The first term on the right gives rise to the elastic scattering while the second term is the perturbation potential used in the DWBA calculations.

A valid test of the surface scattering hypothesis requires that a large range in V_0 be scanned so that values which might refute the hypothesis will not be missed. The range from $V_0=-10$ MeV to $V_0=-80$ MeV was chosen since most present day optical model analyses and distorted wave Born approximation (DWBA) fits use potentials whose real parts lie in this range. The data presented by Drisko *et al.*[11] indicate that varying V_0 in 10-MeV steps should be satisfactory.

The actual technique followed in practice was first to find one set of parameters that would fit the elastic data well in the region from 20 to 120°. For angles

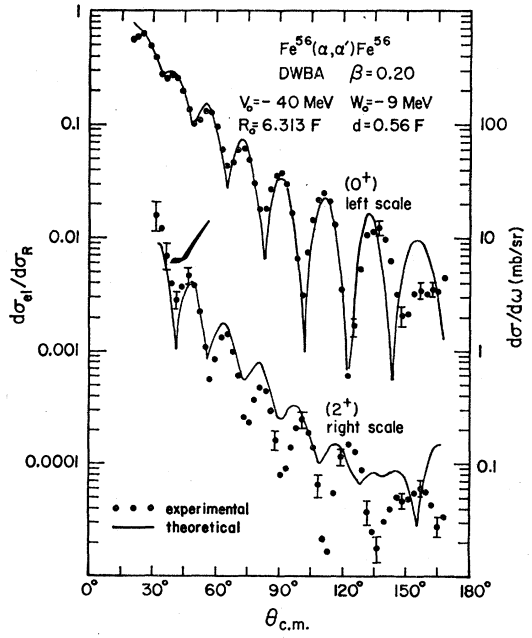

FIG. 10. Experimental and theoretical ($V_0=-70$ MeV) angular distributions for the reaction $Fe^{56}+\alpha$(22.2 MeV).

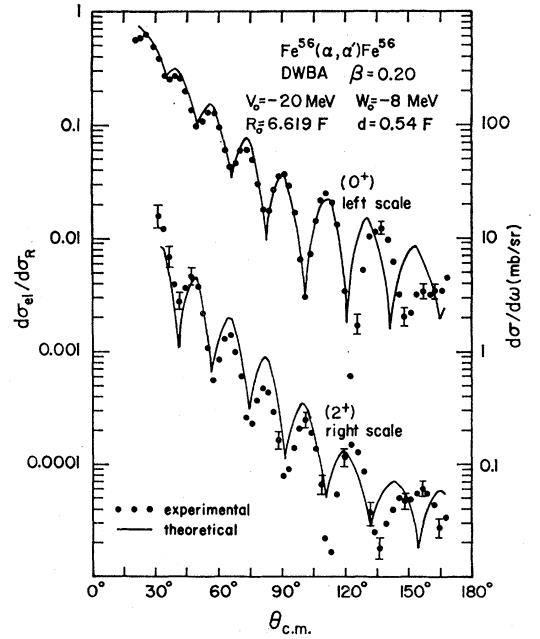

FIG. 12. Experimental and theoretical ($V_0=-20$ MeV) angular distributions for the reaction $Fe^{56}+\alpha$(22.2 MeV).

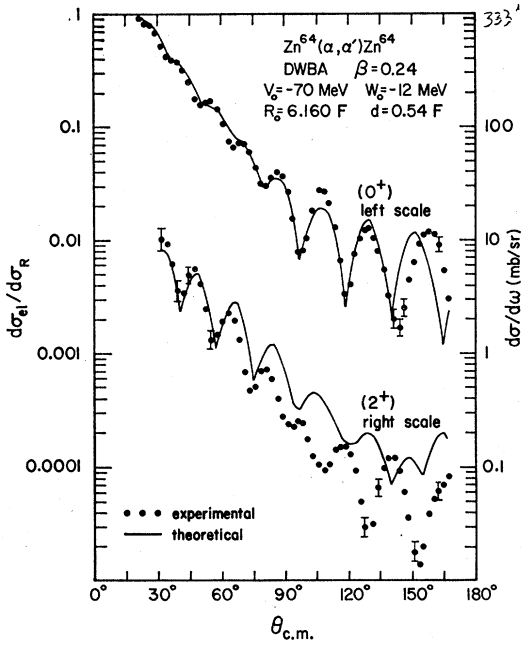

FIG. 13. Experimental and theoretical ($V_0=-70$ MeV) angular distributions for the reaction $Zn^{64}+\alpha$(22.2 MeV).

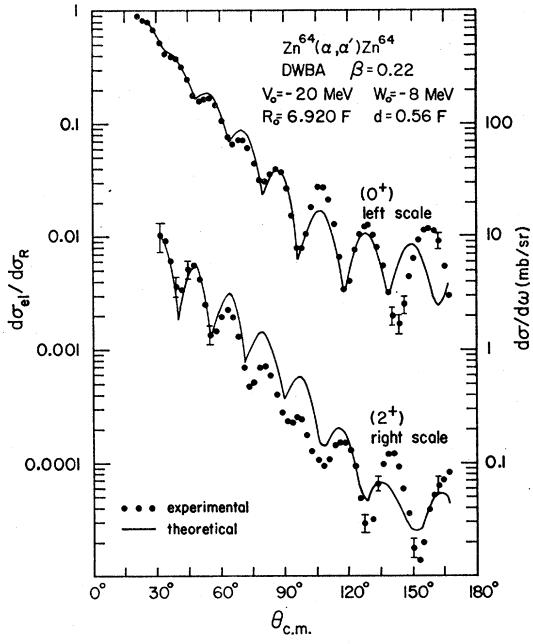

FIG. 15. Experimental and theoretical ($V_0=-20$ MeV) angular distributions for the reaction $Zn^{64}+\alpha$(22.2 MeV).

greater than 120°, the agreement with theory was poor; consequently, these angles were not used in computing χ^2. Once this first "best" set was obtained, it was used to compute C_1. Since a scan was always done over W_0, it was unnecessary to find C_2. V_0 was then varied in 10-MeV steps from -10 to -80 MeV, each time using Eq. (1) to find the appropriate R_0 with d held fixed at the value obtained in the first "best" set. Keeping d fixed will be justified later. Calculations were performed for each value of V_0 using various values of W_0 until a minimum in χ^2 was found.

If it be true that only the surface of the nucleus is effective in the scattering, then it will also be true that

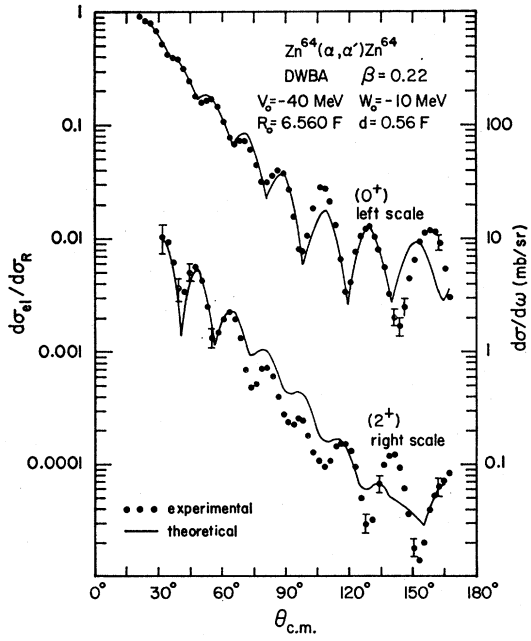

FIG. 14. Experimental and theoretical ($V_0=-40$ MeV) angular distributions for the reaction $Zn^{64}+\alpha$(22.2 MeV).

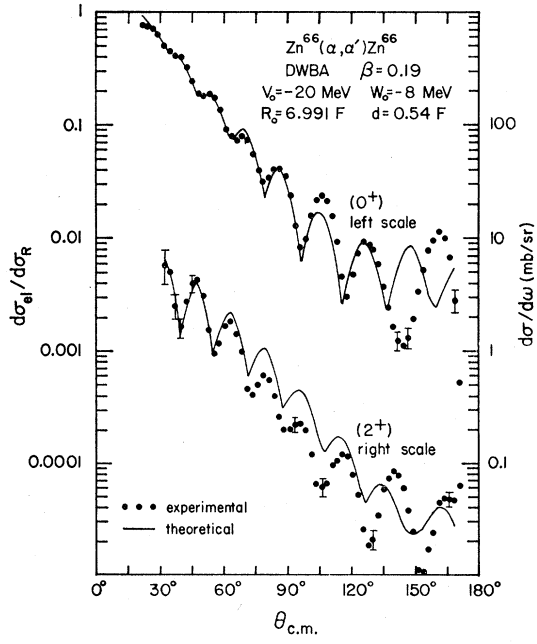

FIG. 16. Experimental and theoretical ($V_0=-20$ MeV) angular distributions for the reaction $Zn^{66}+\alpha$(22.2 MeV).

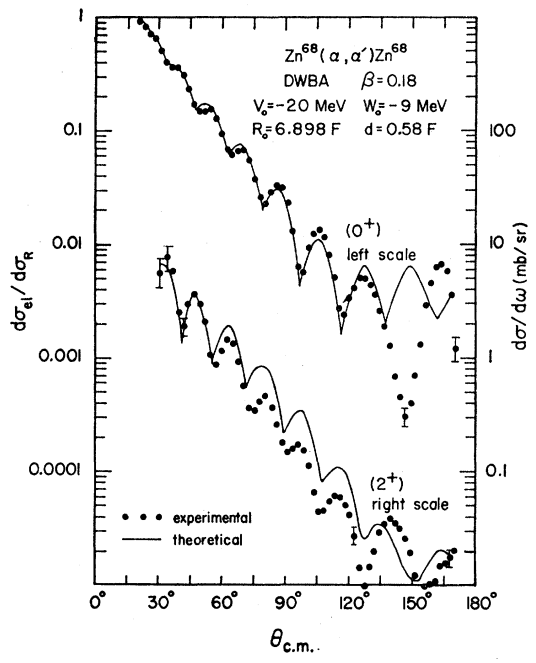

FIG. 17. Experimental and theoretical ($V_0=-20$ MeV) angular distributions for the reaction $Zn^{68}+\alpha(22.2$ MeV).

equally good fits should be obtained for each value of V_0. This was found not to be the case. Distinct minima in χ^2 were found for three values of V_0, viz., $V_0=-20$, -40, and -70 MeV. This can be seen in Fig. 9 which shows a plot of χ^2 (min) versus $-V_0$ for Zn^{68}. The other nuclei studied yielded similar results.

The use of a fixed d was checked by making calculations with the same parameters, except d, which gave the above three minima in χ^2. It was found that in some cases the minima could be decreased very slightly by varying d, but that no significant reduction could be made. It therefore seemed proper, when searching for deep minima, to keep d fixed having once found its approximate value in the original "best" set. For each of the above three V_0's, the final value of d selected (i.e., those appearing in Figs. 10–17) was the one that gave the deepest minima in χ^2.

The above search procedure can be considered correct if one shows that the original "best" set of parameters is indeed a "best" set, i.e., corresponds to a deep minimum in χ^2, otherwise the constant C_1 may be wrong. This means that in seeking the first set of parameters, a range in V_0 must be scanned which is large enough to contain at least one deep minimum. The first set of parameters was obtained by scanning V_0 in 2-MeV steps from -50 to -80 MeV, varying W_0, d, and R_0 each time until the minimum in χ^2 was found. The value of χ^2 (min) found for $V_0=-70$ is therefore indeed a significant minimum, and not just a minor local minimum which might have been obtained for an insufficient range of V_0.

The fact that only three values of V_0 were found to yield deep minima in χ^2 suggests that the interior of the nucleus does play an important role in determining the elastic scattering. Similar results were found recently by Blatchley,[17] who also used the same technique in fitting some $Si^{28}(\alpha,\alpha)Si^{28}$ data.

A further criterion can now be placed on these three sets of parameters by their use in DWBA calculations to see if one will fit the inelastic 2^+ (first excited state) data better than the other two. For each set, DWBA calculations were made for several values of β [the quadrupole distortion parameter, related to $\alpha_{2\mu}$ by $(\beta^2=\sum_\mu \alpha_2{}^2)$] until a β was found which made the first maximum in the theoretical inelastic distribution coincide with the first maximum of the corresponding experimental distribution. The required values of β were found to depend on V_0. However, in all cases they fell between 0.18 and 0.24. The final values of β are given on the figures which display the corresponding fits to the data.

In fitting the Zn^{64} and Zn^{68} elastic data, it was found that at the forward angles ($\leq 90°$) the theoretical values lay consistently above the experimental curve, independent of V_0, although they had the proper structure and slope. In this region, especially for angles less than 45°, the Coulomb scattering is large so that one would expect the theory to be quite accurate. The experimental data were normalized to the theoretical predictions in order to make them more amenable to comparison. The range from 20° to 30° was used to obtain the normalization factors of 1.29 for Zn^{64} and 1.10 for Zn^{68}. These factors are consistent with the errors associated with the absolute cross section determination.

B. Interpretation of Data

Figures 10, 11, and 12 show the fits to the Fe^{56} data for $V_0=-70$, -40, and -30 MeV, respectively. It is apparent from these figures that the fits to the elastic data are essentially equally good. However, it is clear that the best fit to the inelastic 2^+ data is obtained with the set of parameters which includes $V_0=-20$ MeV (Fig. 12). This also agrees with the work of Blatchley,[17] who obtained the best fit to the inelastic 2^+ Si^{28} data with $V_0=-23$ MeV. Moreover, he found that the theory did not predict the experimental angular-correlation pattern except for a value of V_0 in the neighborhood of -20 MeV. No angular-correlation data were taken in this experiment since the theory predicts essentially the same results for each of the three sets of parameters. From Figs. 13, 14, and 15, which show the results for Zn^{64}, it can be seen that the only set of parameters that will produce the proper structure and also give maxima and minima in agreement with the experimental inelastic results is the set containing

[17] D. E. Blatchley, thesis, Indiana University, 1964 (unpublished).

$V_0=-20$ MeV. Similar results were found for Zn^{66} and Zn^{68} so only the best fit for each is shown (Figs. 16 and 17).

One noticeable feature of both the elastic and inelastic distributions is the failure of the theory to fit the back angle data ($\Theta_{c.m.}>120°$ for Fe^{56}, $\Theta_{c.m.}>135°$ for the Zn isotopes). There are at least two explanations that can be offered for this: (a) failure of the simple quadrupole, harmonic, vibrational Hamiltonian to adequately describe the behavior of the nucleus in connection with large momentum transfer events; and (b) the occurrence of compound-nucleus processes, since those particles which are scattered through large angles have penetrated most deeply into the nucleus, thus increasing the probability of compound-nucleus reaction. A deviation from the predictions of direct-reaction theory is therefore to be expected. However, if the disagreement is due to compound-nucleus formation, one would not expect the theoretical predictions to fit the data better merely by adding a smoothly varying compound-nucleus cross section. It would be necessary to add the amplitudes for the two competing processes, direct-reaction and compound-nucleus formation, in order to arrive at a prediction similar to the experimental curve. Some interference effect would be necessary to reproduce the minima at about 145° in the Zn elastic distributions (e.g., Figs. 15, 16, and 17). It is also clear that in the Fe^{56} elastic distribution (Fig. 12), the addition of a compound-nucleus cross section to the cross section predicted by a direct-reaction theory would make the fit worse.

Another interesting fact is that the peak-to-valley ratio for the last peak (at approximately 162°) in the Zn elastic distributions, becomes progressively larger as A increases. The height of the last peak relative to the preceding one also increases with A. In Fe^{56}, on the other hand, the last peak in the elastic distribution is absent. How these effects are related to shell structure is not known at the present time.

The experimental inelastic 2^+ Fe^{56} distribution is approximately 90° out of phase with the elastic distribution in the angular range from 30 to 135°. The theoretical prediction for the inelastic distribution is also 90° out of phase with the predicted elastic distribution; this is consistent with the Blair phase rule.[18] Only for the set of parameters with $V_0=-20$ MeV is the 90° phase relation maintained over the entire angular range (Fig. 12). Similar results are obtained for the Zn isotopes except that the experimental data obey the phase rule better at the back angles than did the Fe^{56} data, see Figs. 15, 16, and 17.

It is also of interest to compare the experimental Fe^{56} inelastic 2^+ distribution with the corresponding Zn distributions. The oscillations are larger (peak-to-valley) for Fe^{56} than for the Zn isotopes. They are also quite uniform to nearly 130°. In the Zn distributions the oscillatory pattern is considerably damped at about 95° compared to the peaks on either side. This is not the case for Fe^{56}. If we now re-examine the best fits to the elastic data, Figs. 12, 15, 16, and 17, it is clear that they are not as good in the range from 95 to 110° for the Zn isotopes as for Fe^{56}. It may be that the diminution of the Zn 2^+ peaks in this region leads to an accentuation of the elastic peaks which in turn causes the poor fits between 95 and 110°.

TABLE III. Comparison of results.

Nucleus	Bombarding particles and their energies in MeV	$(B(E2)/e^2)$ (10^{-49}cm^4)	β	Reference
Fe^{56}	N(16.3; 36)	0.61		a
	α(6–7)	1.10±0.16	0.24	b
	α(22.2)	0.74±0.15	0.20	This work
Zn^{64}	N(36.0)	1.10		a
	α(?)	0.83		a
	α(6–7)	1.10±0.16	0.20	b
	α(22.2)	1.51±0.30	0.22	This work
	α(7.0)	1.70±0.15	0.252	c
Zn^{66}	N(36.0)	1.10		a
	α(?)	0.89		a
	α(6–7)	0.87±0.13	0.17	a
	α(5.5)	1.45±0.13	0.227	c
	α(22.2)	1.19±0.24	0.19	This work
Zn^{68}	N(36.0)	1.10		a
	α(?)	0.84		a
	α(5.5)	1.25±0.11	0.206	c
	α(22.2)	0.99±0.18	0.18	This work

[a] D. S. Andreyer, A. P. Grinberg, K. I. Erokhina, and I. Kh. Lemberg, Nucl. Phys. 19, 400 (1960).
[b] See Ref. 19.
[c] P. H. Stelson and F. K. McGowan, Nucl. Phys. 32, 652 (1962).

Finally, we can compare the present results for β, the quadrupole deformation parameters, and $B(E2)$, the electric quadrupole-transition probability between the ground and first 2^+ state, with electromagnetic results. These values and the results from this work, are collected in Table III. In this table, N in the bombarding particle column refers to nitrogen ions. Comparison shows that the values obtained for $B(E2)$ in this work are consistent with the electromagnetic values to within the errors, where assigned. The $B(E2)$ values calculated on the basis of the data presented in this paper were obtained from the equation

$$B(E2)=\beta^2(\tfrac{3}{4}\pi ZeR_N^2)^2. \tag{8}$$

The R_N's were obtained from the T_0's (see Figs. 12, 15, 16, and 17) by subtracting the alpha-particle radius. This was done by finding an r_0 such that

$$\begin{aligned} R&=r_0A_N^{1/3}+r_0A_\alpha^{1/3}, \\ &=R_N+R_\alpha. \end{aligned} \tag{9}$$

A value of 1.23±0.02 F was found for r_0 when an average was taken for the four nuclei studied.

[18] J. S. Blair, Phys. Rev. 115, 928 (1959).

The electromagnetic values for β are seen to be slightly larger than the values obtained by alpha-particle scattering, both for the Zn isotopes and for Fe^{56}. The electromagnetic value of β was determined for Fe^{56} by Temmer and Heydenburg[19] to be approximately 0.24. Buck[20] had obtained the values 0.24 and 0.21, respectively, from the analysis of the inelastic scattering of 14.3- and 17.4-MeV protons from Fe^{56}. The β values which he obtains by analysis of the inelastic scattering of 11.1-MeV protons by Zn^{64}, Zn^{66}, and Zn^{68} are 0.27, 0.23, and 0.20, respectively. The β value which we find for Fe^{56}, 0.20, is in good agreement with the 0.21 value reported by Buck. However, the values which we obtain for the Zn isotopes are consistently smaller than those found by Buck. It should be emphasized that our values were obtained using projectiles with considerably more energy than those used in Buck's analyses except for the case of 17.3-MeV protons on Fe^{56}, which was in good agreement with our value.

C. Discussion

The calculations made here show the large-angle scattering cross sections to be very sensitive to changes in the interaction potential used. Agreement with the experimental data at the larger angles would require several refinements in the calculations. A more realistic model for the target nucleus could well be used, as the only justification for the quadrupole harmonic vibrator model is one of computational simplicity.

The use of a volume-absorption, optical-model potential in which the real and imaginary parts have a common diffuseness parameter and a common radius is an approximation. To what extent this affects the conclusions drawn here is unknown. No thorough search has been made, as yet, using various other potentials, e.g., surface absorption. The possibility of using a volume-absorption potential with real and imaginary parts having unequal radii and unequal diffuseness parameters also might well be investigated.

The effects of Coulomb excitation have been neglected here. Bassel *et al.*[21] show that for 43-MeV alpha particles on Ni^{58}, the effect of this mode of excitation is negligible, but, at 18 MeV they find that Coulomb excitation has become important especially for scattering angles less than about 45°. They also show that distortion of the incoming and outgoing waves by the optical potential and the Coulomb potential tends to reduce the effect of Coulomb excitation at angles greater than 45° compared to the case in which the waves are distorted only by the Coulomb field. For 22-MeV alpha particles, we would also expect Coulomb excitation to be most significant at the far forward angles.

An approximation which was capable of verification concerns the use of the DWBA. Its validity was tested by a coupled channels calculation for Zn^{64} in which coupling from the first excited state back into the ground state was explicitly taken into account. The results were found to be very nearly identical to those predicted by the DWBA.

Finally, it should be emphasized that we have used local potentials and have neglected contributions from exchange between projectile and target nucleus due to (anti-) symmetrization. The effect which this has on the predicted angular distributions is not known.

V. CONCLUSIONS

Results are presented which indicate that the predictions of the DWBA for the inelastic scattering of 22-MeV alpha particles are sensitive to the real part of the optical potential. It is shown that, within the framework of the collective model, and under the restrictions set down in the previous section, this sensitivity can be used to reduce the ambiguity which arises in the optical potential when only the elastic data are analyzed. The results also show that these conclusions could not have been drawn if data had only been taken to, say, 70°.

At large angles ($\geq 130°$) the agreement with theory for both the elastic and inelastic data is poor. Two explanations have been proposed for this failure: (a) breakdown of the nuclear model, and (b) the occurrence of compound-nucleus reactions. It has been argued that if the latter is true, then we must add amplitudes rather than cross sections.

Finally, it is possible, by fitting the inelastic data, to obtain $B(E2)$ values which are in agreement with the electromagnetic values.

ACKNOWLEDGMENTS

The authors would like to express their appreciation to Dr. J. G. Wills for making his code available and for the time which he gave so generously in discussing the results. The help of Charles Foster, Gorden Eckley, and Steve Robinson in recording data is acknowledged.

[19] G. M. Temmer and N. P. Heydenburg, Phys. Rev. **104**, 967 (1956).
[20] B. Buck, Phys. Rev. **90**, 712 (1962).
[21] R. H. Bassel, G. R. Satchler, R. M. Drisko, and E. Rost, Phys. Rev. **128** 2693 (1962).